

**Study on the Various Geometry Configurations of a Microchannel for
Ammonia Synthesis**

by

Shafiq Iqbal Bin Mohd Amadin
13373

Dissertation submitted in partial fulfilment of
the requirements for the
Bachelor of Engineering (Hons)
(Chemical Engineering)

JANUARY 2014

Universiti Teknologi PETRONAS
Bandar Seri Iskandar
31750 Tronoh
Perak Darul Ridzuan

CERTIFICATION OF APPROVAL

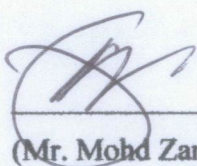
Study on the Various Geometry Configurations of a Microchannel for Ammonia Synthesis

by

Shafiq Iqbal Bin Mohd Amadin
13373

A project dissertation submitted to the
Chemical Engineering Programme
Universiti Teknologi PETRONAS
in partial fulfilment of the requirement for the
BACHELOR OF ENGINEERING (Hons)
(CHEMICAL ENGINEERING)

Approved by,



(Mr. Mohd Zamri Bin Abdullah)

UNIVERSITI TEKNOLOGI PETRONAS
TRONOH, PERAK
January 2014

CERTIFICATION OF ORIGINALITY

This is to certify that I am responsible for the work submitted in this project, that the original work is my own except as specified in the references and acknowledgements, and that the original work contained herein have not been undertaken or done by unspecified sources or persons.



SHAFIQ IQBAL BIN MOHD AMADIN

ABSTRACT

The conventional method to produce ammonia employs the Haber–Bosch process at high pressure and temperature with aid of iron or iron oxide catalyst. These working conditions not only consumes tremendous amount of energy, it has higher safety risk, in addition to not achieving very high conversion and yield. OneBaja project offers a new method to synthesize ammonia which is via microreactor at ambient operating conditions with the aid of magnetic induction and facilitated by catalyst. Prior to study on microreactor, it is essential to understand the hydrodynamics of flow in microchannel. This study aims to investigate the hydrodynamics of the mixing of nitrogen and hydrogen gases in various geometry configurations of a microchannel in order to embed the catalyst for the ammonia synthesis at the uttermost optimum location. Computational Fluid Dynamics simulation will be employed to simulate the mixing of nitrogen and hydrogen gases whereby the results from will serve as a stepping point to design a microreactor for the ammonia synthesis.

ACKNOWLEDGEMENTS

First and foremost, I would like to give praises to the Allah the Almighty for the opportunity to complete this project. The completion of this project would not be possible without the supports of many individuals. Thus, I would like to extend my gratitude and acknowledgements to all of them who had been directly and indirectly involved in this project.

I am highly indebted to my final year project supervisor, Mr Mohd Zamri Bin Abdullah for giving me the opportunity to carry out this project under his supervision. His exemplary guidance and supervision especially when I have doubts and inquiries regarding the project are most invaluable and valued. Moreover, his willingness and patience to spend time from his busy working schedule is indeed most appreciated. The constant help and encouragement had really helped me a lot during the accomplishment of the project.

I would also like to take this opportunity to thank both the coordinators for Final Year Project I and II for all their hard work coordinating the courses. Their dedication to organize talks has been most helpful with the accomplishment of the project. I also would like to thank all the postgraduate students who had helped to guide me in doing this project.

Besides, I am entirely grateful with my fellow course mates for their continuous support and willingness to help me out with their abilities during the period of my project. Lastly, I would like to express my special gratitude to my family and friends for being my strong pillars of encouragement.

TABLE OF CONTENTS

CERTIFICATION OF APPROVAL	i
CERTIFICATION OF ORIGINALITY	ii
ABSTRACT	iii
ACKNOWLEDGEMENT	iv
TABLE OF CONTENTS	v
LIST OF FIGURES	vi
LIST OF TABLES	vii
CHAPTER 1: INTRODUCTION	1
CHAPTER 2: LITERATURE REVIEW AND THEORY	
2.1 Microtechnology	4
2.2 Computational Fluid Dynamics	9
2.3 Related Studies	9
CHAPTER 3: METHODOLOGY	
3.1 Research Methodology	16
3.2 Tools	23
3.3 Key Milestone	23
CHAPTER 4: RESULTS AND DISCUSSION	
4.1 Mesh Sensitivity Study	24
4.2 Velocity of Gas Components in Microchannel	29
4.3 Pressure Drop Across Microchannel	36
CHAPTER 5: CONCLUSION AND RECOMMENDATIONS	38
REFERENCES	40
APPENDICES	44

LIST OF FIGURES

Figure 1	Design of Micromixer with Chaotic Advection (Nguyen and Wu, 2005)	7
Figure 2	Schematic of micromixing problem geometry (Yan and Farouk, 2001)	10
Figure 3	Zig-zag microchannel with "Y" inlet junction (Mengeaud et al., 2002)	10
Figure 4	Schematic of Mixing Problem Geometry and Conditions (Wang and Li, 2006)	11
Figure 5	Mixing length variation for various main flow velocities for $T = 300\text{K}$ (Wang and Li, 2006)	11
Figure 6	Mixing length variation for various main flow temperatures for $V = 106\text{ m/s}$ (Wang and Li, 2006)	11
Figure 7	Scheme of studied geometry (Reyhanian et al, 2011)	12
Figure 8	Schematic of the setup showing the channel model. (a) is the channel model with an one-period mixing unit, (b) is the detailed design of the mixing unit, (c) is the mixing unit with n periods. (Fang et al, 2012)	13
Figure 9	Comparison of the grey images from the computer simulations (a), (c), (e) and the experiments (b), (d), (f). (a) and (b) are the "T" inlet channel, (c) and (d) contain a one-period mixing unit, (e) and (f) contain a 28-period mixing unit, (f) shows part of the mixing features because of the limitation of the microscope field. The arrows indicate the flow direction. (Fang et al, 2012)	13
Figure 10	Geometry of Microchannel (Rosli, 2012)	14
Figure 11	Various Inlet Configurations (Azeman, 2012)	15
Figure 12	Geometry Configuration A	17
Figure 13	Geometry Configuration B	18
Figure 14	Boundary Conditions	19

Figure 15	Mesh 1 Design A	24
Figure 16	Mesh 1 Design B	25
Figure 17	Mesh 2 Design B	25
Figure 18	Location of Comparison	26
Figure 19	Nitrogen velocity profile	28
Figure 20	Axial Hydrogen Velocity for Design A	29
Figure 21	Radial Hydrogen Velocity for Design A	30
Figure 22	Axial Nitrogen Velocity for Design A	30
Figure 23	Radial Nitrogen Velocity for Design A	31
Figure 24	Segment of Microchannel Design A	31
Figure 25	Axial Hydrogen Velocity for Design B	33
Figure 26	Radial Hydrogen Velocity for Design B	33
Figure 27	Axial Nitrogen Velocity for Design B	34
Figure 28	Radial Nitrogen Velocity for Design B	34
Figure 29	Pressure Profile along the Microchannel	37
Figure 30	Mesh with 3694695 nodes	46
Figure 31	Mesh with 4512733 nodes	46
Figure 32	Mesh with 4911049 nodes	47

LIST OF TABLES

Table 1	Classification Scheme of Micromixers (Nguyen, 2008)	7
Table 2	Variables Manipulated in Simulation (Rosli, 2012)	14
Table 3	Domain Physics	19
Table 4	Boundary Physics	20
Table 5	Solver Control	21
Table 6	Completed Meshing Properties	26
Table 7	Comparison of velocity contour plot	27

CHAPTER 1

INTRODUCTION

1. INTRODUCTION

Elemental nitrogen, N is an essential component required by all living organism to build proteins and DNA. However, nitrogen exists as a diatomic molecule. Two nitrogen atoms are bonded by a strong triple bond making it relatively inert. In order for living organisms to be able to use nitrogen, N₂ gas must first be turned into a molecule that can be assimilated readily by plants (Schrock, 2006). Hence, the molecule is called ammonia, NH₃. Ammonia can be converted into ammonium, NH₄⁺, nitrite, NO₂, nitrate, NO₃ or organic nitrogen such as urea, NH₂CONH₂ (Harrison, 2003).

Ammonia was first commercially synthesized in 1870 through the Haber–Bosch process. This synthesis method was patented by German chemist, Fritz Haber on 13 October 1908 and applied in the industry by his colleague Carl Bosch in 1913. Haber process involves the reaction between nitrogen and hydrogen at elevated temperature and pressure in the presence of a catalyst consisting of a mixture of iron and iron oxide. Due to the technology at that time was unable to cater the high temperature and pressure required by the process, Carl Bosch succeeds in inventing an apparatus that was capable to handle such condition. His innovation led to the development of high pressure reactors. Ammonia synthesis via Haber–Bosch process requires a working condition at pressure of 200–400atm and temperature of 400–600°C. Worldwide, the Haber – Bosch process is used to produce more than 500 million metric tonnes of ammonia of which 80% is being used to produce fertilizers (Potashcorp.com, 2013).

Due to the high-pressure synthesis condition required by Haber–Bosch process, it consumes tremendous amount of energy. The process consumes an estimated of 1% of the world energy consumption (Schrock, 2006; Visionlearning, 2003). Besides that, Dr. Jürgen Korkhaus, Head of Materials Engineering at BASF SE explains, “Even today, the industrial production of ammonia is still operating at the limits of the possible. The challenges for the material and technology of the production plant are enormous under these high pressure synthesis conditions,” when he compared the present with past practice (BASF SE, 2013). Not only Haber–Bosch process impose high cost to produce ammonia, the high pressure working condition also requires extra safety and control regulation in operating the plant. Moreover, due to the exothermic nature of the reaction, the operating temperature for the reaction was compensated such that it only yield approximately 30% conversion of reactants into products.

Due to these issues, OneBAJA program was introduced to investigate a new method for synthesizing ammonia and urea. This method, called green urea production aims to be more economical, energy saving and lower operational risk. This method involves design of a new synthesis route that could enhance the process and performance, respectively. In this program, ammonia will be synthesized at ambient operating condition by the means of magnetic induction zone to produce a higher ammonia yield compared to the conventional Haber–Bosch. Thus, catalyst plays an important role to facilitate the process. This reaction would be conducted inside a microreactor. In this project, Computational Fluid Dynamics (CFD) will be employed to design this new reactor.

On the other hand, as the application of microfluidic technology is still relatively new, there is no definite way of designing microreactor. Before proceeding to fabrication of the new microreactor, an optimum design of microchannel that is capable of effective mixing is required. As ineffective mixing might occur in microchannel due to the laminar flow behavior of the fluid in microfluidic device, studies must first be conducted to identify the parameter that affects its mixing ability. Adequate mixing is an essential

requirement for propulsion devices designed to provide chemical reaction and heat release in streams of gas and fuel (Yan and Farouk, 2001).

As the current stage disregards the reaction between nitrogen and hydrogen that lead to the synthesis of ammonia, the objective of this project is to study the hydrodynamics of mixing between the two reactant gases in various geometry configurations of a microchannel. The purpose is to determine a suitable location to embed the catalyst for ammonia synthesis, which is what the next stage of the project will commence.

The simulation covers the hydrodynamics of the mixing behavior of the two reactant gases in various geometry configuration of the microchannel in microfluidic environment. The simulation is conducted through the use of ANSYS CFX 14.5 software. The parameter of the microchannel that is varied is mainly the geometry configuration. It is expected through this study, an optimum design will be achieved that will predict optimum mixing behaviour that will enable the localization of the catalyst in the microreactor for reaction producing ammonia.

CHAPTER 2

LITERATURE REVIEW AND THEORY

2. LITERATURE REVIEW AND THEORY

2.1 Microtechnology

The prefix “micro” generally designates chemical systems fabricated with techniques originally developed for electronic circuits (Jensen, 2001). Microfabrication for chemical systems is a field that started by using fabrication techniques developed for microelectronics to construct sensors and actuators, but now encompasses a wide range of materials and fabrication methods (Jensen, 2001). Microfluidics can have a revolutionary impact on chemical analysis and synthesis, similar to impact of integrated circuits on computers and electronics (Nguyen and Wereley, 2006). With microsystems, it is possible to increase the yield in certain chemical reactions dramatically and at the same time reduce the realization of byproducts (Koch et al., 2000).

Mixing is the central process of most microfluidic devices for medical diagnostics, genetic sequencing, chemistry production, drug discovery and proteomics (Jensen, 2001). Mixing is a transport process for species, temperature, and phases to reduce in homogeneity (Nguyen, 2008). It leads to secondary effects such as reaction and change in properties. There are three established terminologies for mixing which are macromixing, micromixing and mesomixing. Macromixing refers to mixing governed by the largest scale of fluid motion, while micromixing is the smallest scale of fluid motion and molecular motion. Mesomixing, on the other hand, is the scale between macromixing and micromixing.

Turbulent flow is generally preferred in a channel if intimate mixing is desired between two streams (Mills et al., 2007). At a macroscale level, mixing is conventionally achieved by a turbulent flow, which makes possible the segregation of the fluid in small domains, thereby leading to an increase in the contact surface and decrease in the mixing path. Mixing in microfluidic devices is generally achieved by taking advantage of the relevant small length, which dramatically increases the effect of diffusion and advection (Capretto et al., 2011).

Microfluidic devices are not merely a miniature version of their macroscale counterpart because of many physical characteristics, such as surface area-to-volume ratio, surface tension and diffusion are not linearly proportional from large to small devices. Microfluidic mixer should be designed in such ways that leverage the physical characteristic of the mixing in a confined space (Capretto et al., 2011).

One of the operating parameters paid attention to in study of micromixing is the Reynolds Number which represents the ratio between momentum and viscous friction. The Reynolds Number is defined as:

$$Re = \frac{\rho v D_H}{\mu} \quad (1)$$

Where

v = flow velocity;

ρ = fluid density;

D_H = hydraulic diameter;

μ = dynamic viscosity.

For microfluidic systems, Reynolds number, Re are typically smaller than 100 and the flow is considered essentially laminar (Nguyen and Wu, 2005). This characteristic has a direct consequence on mixing within microfluidic devices. In an environment where the fluid flow is restrictedly laminar, mixing is largely dominated by passive molecular diffusion and advection. Diffusion is defined as the process of spreading molecules from

a region of higher concentration to one of lower concentration by Brownian motion, which results in a gradual mixing of material (Capretto et al., 2011).

The aim of microfluidic mixing schemes is to enhance the mixing efficiency such that a thorough mixing performance can be achieved within shorter mixing channels, which can reduce the characteristic size of microfluidic devices (Lee et al., 2011). Micromixers are generally designed with channel geometries that decrease the mixing path and increase the contact surface area. Common channel widths are on the order of 100 to 500 μm while the length could be a few millimetres or more (Nguyen, 2008). Designing micromixers relies on manipulating the flow using channel geometry or external disturbances (Nguyen, 2008). General requirements for micromixers are:

- Fast mixing time
- Small device area
- Integration ability in a more complex system

There are two types of micromixers as categorized by Nguyen and Wu (2005) which are active and passive micromixers. Passive micromixers do not have moving parts and hence, do not require external energy. The mixing process relies entirely on molecular diffusion or chaotic advection. In active mixers, moving parts are involved. It utilizes disturbance provided by external fields for mixing process. Generally, active mixers have higher efficiencies. However, due to requirement for integration of peripherals such as actuators and power source it is more complex and expensive to fabricate. Thus, passive mixers are more favourable to be applied in microfluidic systems.

Table below shows the classification scheme of micromixers.

TABLE 1: Classification Scheme of Micromixers (Nguyen, 2008)

Active	Passive
Pressure Disturbance	Lamination
Electrohydrodynamic	Injection
Dielectrophoretic	Chaotic advection
Electrokinetic	Droplet
Magnetohydrodynamic	
Acoustic	
Thermal	

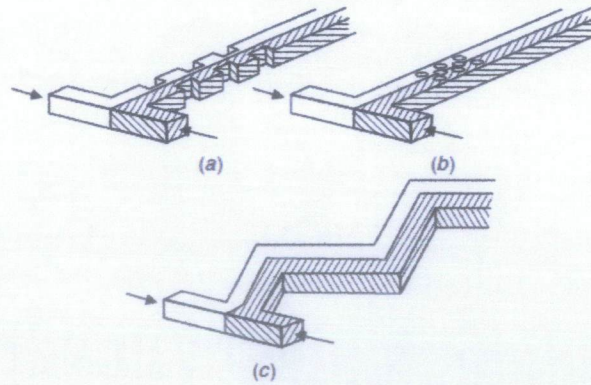


Figure 1 Design of Micromixer with Chaotic Advection (Nguyen and Wu, 2005)

According to Aubin et al. (2005), there are no common rules to design micromixer. They further added that microreactors are merely continuous laminar flow reactors and the design approach for micromixing should be dealt with similar manner to laminar mixing in macro-scale pipe flow. In this project, passive micromixer based on chaotic advection is selected as a reference to design this microchannel. The basic design concept for the generation of advection is the modification of the channel shape for stretching, folding, and breaking of the laminar flow (Nguyen, 2008). During chaotic advection, the streamlines should cross each other at different times. The aim for the design is such that to provide sufficient spatial and temporal mixing as fast as possible (Aubin et al., 2005).

Microreactors are networks of micron to millimetre-sized channels typically etched into a solid substrate where only small volumes of chemicals react at a given time. For a reaction engineer, the term “microreactor” traditionally has meant a small tubular reactor for testing catalyst performance (Jensen, 2001). The high heat and mass transfer rates possible in microfluidic system allow reactions to be performed under more aggressive conditions with higher yields than can be achieved with conventional reactors (Jensen, 2001). Besides that, it also allows reactions to be performed under more uniform temperature conditions.

Microreactors are also much safer compared to their macro counterparts. In the event of failure where chemicals are accidentally released, it could be easily contained due to its small quantity. Moreover, the presence of integrated sensor and control units could allow the failed reactor to be isolated and replaced while other parallel units continue production. Economically, experimentation at the conventional bench scale is limited by high costs of reagents and safety concerns. All these issues are effectively eliminated by the characteristics of microreactors. The introduction of new chemicals is usually limited due to the risk and high capital costs of scaling from laboratory to production plant. However, by scaling up the production by replications of microreactors used, it would eliminate the costly redesign and pilot plants experiments. The strategy would allow for scheduled gradual investment in new chemical production facilities without committing to a large production facility from the outset. Hence, these circumstances would allow rapid advancement in research and development in new products and technology.

The emergence of microreaction technology and process miniaturization over the past decade has provided a potentially new platform for accelerating the development of these new generation catalysts and multiphase catalytic process technologies (Mills et al., 2007). Once these systems achieve the same reliability as their macroscopic counterparts and offer better cost/performance values, it is expected that the booming markets of biotechnology, analytical and clinical chemistry will also create a booming industry in microfluidics (Koch et al., 2000).

2.2 Computational Fluid Dynamics

Computational Fluid Dynamics is the science of predicting fluid flow, heat transfer, chemical reaction and other related phenomena by solving numerical set of Navier–Stokes equation. The results from CFD analysis are relevant for conceptual studies of new design, detail product development, troubleshooting and redesign.

According to Wang et al. (2003), for microfluidics, there is still no generally accepted experimental method to measure the microfluidic flow field. Thus, numerical simulation is regarded as the critical alternative for the design and performance prediction of microfluidic devices, and compared to experimentation. After running CFD simulation, the result can be evaluated and the parameters can be changed accordingly. The iteration process continues until the microchannel is optimized for certain requirements of microfluidic design, which in this project is to increase the mixing performance. Simulations not only serve as a design tool, but also as a means to interpret experimental data (Quiram et al., 2013). CFD simulation is being used in this project because it is cost-saving, timely, safe and easy to scale-up.

2.3 Related Studies

Yan and Farouk (2001) studied the prediction of mixing of two parallel gas streams in a microchannel by examining effects of inlet velocity, the inlet – outlet pressure difference and the pressure ratio of incoming ratio of the incoming streams on the mixing length. According to the authors, mixing of gas streams is an area of intense research in continuum fluid flow and heat transfer. The mixing in microchannel was simulated with of two parallel gas streams O_2 and H_2 entering at different inlet pressures and inlet streamwise velocities based on the following schematic of micromixing problem geometry.

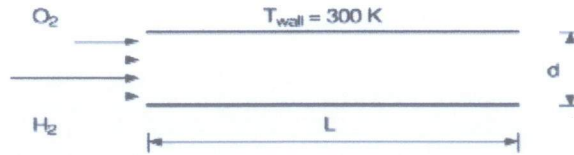


Figure 2 Schematic of micromixing problem geometry (Yan and Farouk, 2001)

They evaluated mixing length of the two gases based on mass density contours and established a relationship between mixing length versus inlet–outlet pressure difference, inlet pressure ratio and velocity for specific geometry and physical conditions.

Mengeaud et al (2002) used the finite element model to study the mixing process of species in a zigzag microchannel integrating a “Y” inlet junction. In order to achieve rapid and homogeneous mixing in microchannel, they employed numerical simulations in order to study mixing effects induced by recirculation phenomena characterized along a zigzag channel as shown.

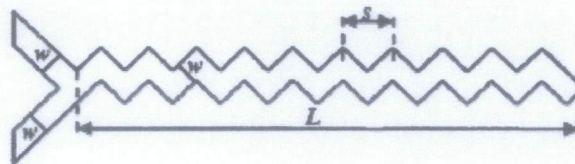


Figure 3 Zig-zag microchannel with "Y" inlet junction (Mengeaud et al., 2002)

The authors found out that linear recirculation induced by the zigzag angles at high flow rates and $Re > 80$ improves mixing process compared to equivalent straight channel. For $Re < 80$, mixing is only ensured by molecular diffusion. They also suggested further studies on the effect of narrowing the zigzag angle value and effect of recirculation on chemical reaction's efficiency.

Wang and Li, (2006) in their study analyzed the inherent factors affecting micro gas mixing. In this study the mixing of two components gas streams were investigated using DSMC method. The analysis simulated two parallel gas streams entering a microchannel separated by a splitter plate for various working conditions. Parameters such as various wall characteristics, inlet gas velocities (50–200 m/s) and gas temperatures

(200 – 400 K) were tested to verify their influences on mixing process. Following figure illustrates the schematic of mixing problem geometry and conditions

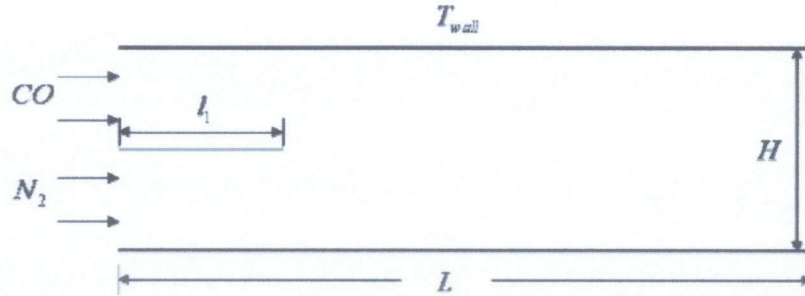


Figure 4 Schematic of Mixing Problem Geometry and Conditions (Wang and Li, 2006)

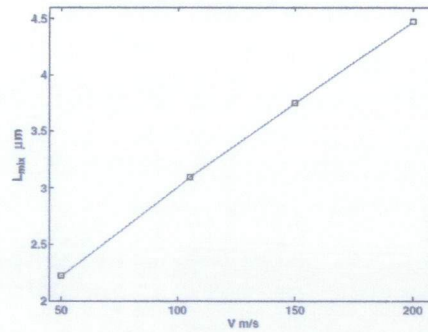


Figure 5 Mixing length variation for various main flow velocities for T = 300K (Wang and Li, 2006)

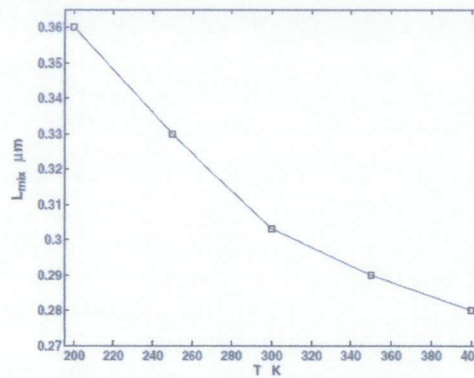


Figure 6 Mixing length variation for various main flow temperatures for V = 106 m/s (Wang and Li, 2006)

The results from the study show that the main flow velocity and temperature were the most important factors affecting the micro gas mixing. The mixing length increases proportionally with inlet velocity but decreases with temperature. Although the wall characteristics do affect the velocity and temperature profiles, the effect on the mixing length is limited.

The study on mixing length in microchannel was also conducted by Reyhanian et al (2011). In their paper, mixing of two parallel gas streams of CO and N₂ with the same inlet boundary conditions in terms of velocity, pressure and temperature is analyzed from DSMC simulations. Similar microchannel as studied by Yan and Farouk (2001) is utilized with addition of bumps near the inlet as shown below.

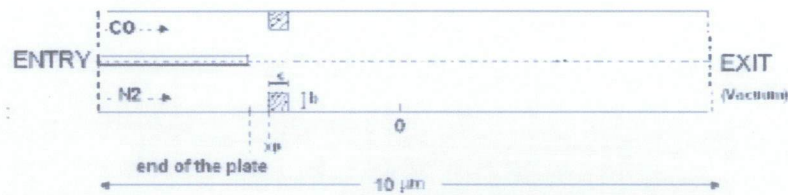


Figure 7 Scheme of studied geometry (Reyhanian et al, 2011)

Parameter studied includes bump height and inlet velocity variation as well as bump effect on the gas mixture pressure. The evaluated mixing by introducing a dimensionless mixing parameter ξ and mixing is achieved when ξ is lower than 2%.

Another study on microchannel was conducted by Fang et al. (2013) where a microchannel comprising a mixing unit embedded with geometric features is designed to enhance mixing. In this study, both simulation and experiments were conducted on two types of liquid. The microchannel device contains a “T” type inlet channel and a mixing unit consisted of simple geometric features which were staggered bars in a mixing unit and produced by wet etching process in a piece of glass during the fabrication of the channel. The CFD simulation was conducted using Fluent 6 (Fluent Inc., Lebanon, NH). Following figure shows the channel structure designed for the simulation.

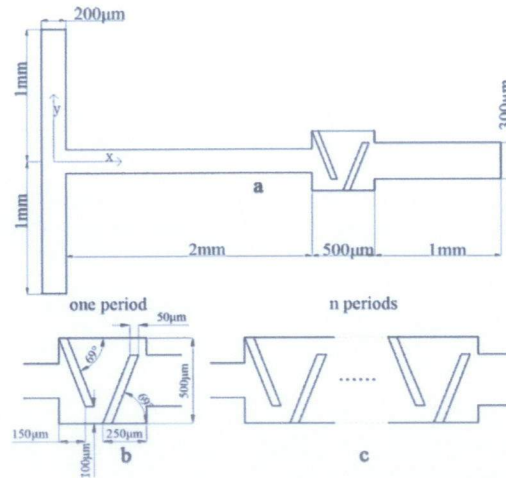


Figure 8 Schematic of the setup showing the channel model. (a) is the channel model with an one-period mixing unit, (b) is the detailed design of the mixing unit, (c) is the mixing unit with n periods. (Fang et al, 2012)

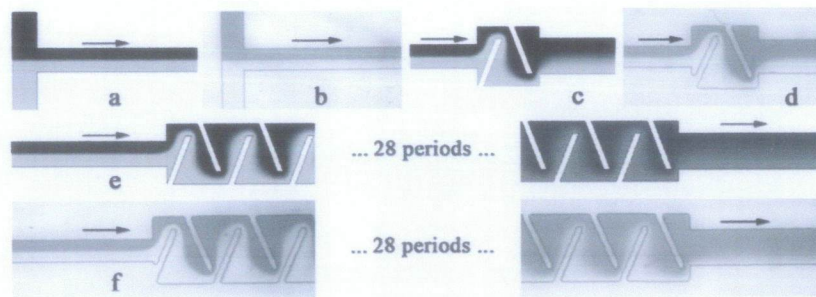


Figure 9 Comparison of the grey images from the computer simulations (a), (c), (e) and the experiments (b), (d), (f). (a) and (b) are the “T” inlet channel, (c) and (d) contain a contain a one-period mixing unit, (e) and (f) contain a 28-period mixing unit, (f) shows part of the mixing features because of the limitation of the microscope field. The arrows indicate the flow direction. (Fang et al, 2012)

Figure above shows the comparison between images from computer simulation and experiment. It was found that concentration distribution for both simulation and experiment are almost similar showing agreement between the two methods. It was also concluded that more period of mixing unit enhances mixing.

For this project, geometric reference will be based on previous work done by Rosli (2012), Azeman (2012) and Liaw (2013). Rosli (2012) study was based on microchannel

geometry as shown below. Different geometries were developed varying in pitch height and number of cycles as summarized in Table 3.

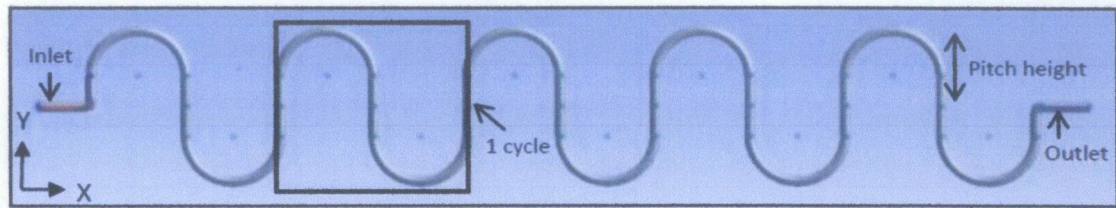


Figure 10 Geometry of Microchannel (Rosli, 2012)

Table 2 Variables Manipulated in Simulation (Rosli, 2012)

Design	Pitch Height	No. of Cycle
I	0.25 cm	3
II	0.25 cm	5
III	0.15 cm	5

It was concluded from the simulation that optimum mixing will be achieved when the number of cycle is 5 at pitch height of 0.15 cm as the fluid flow is stable at that condition.

Continuing his work, Azeman (2012) performed simulation study on Y-inlet microchannel. Two parameters were studied which are the angle of Y-inlet and inflow configuration. The following figure illustrates the different Y-inlet geometry and inflow configuration used in his study.

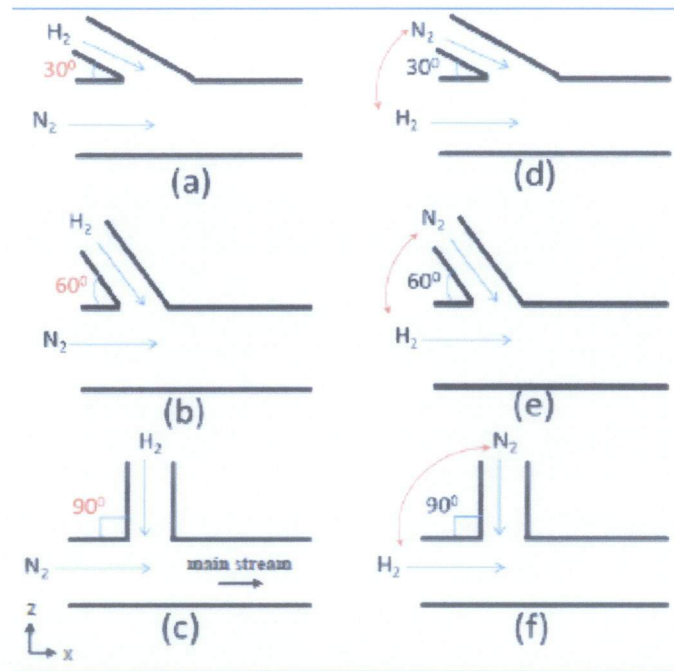


Figure 11 Various Inlet Configurations (Azeman, 2012)

He concluded that design with 30° inlet stream with hydrogen as the main stream resulted in the best mixing performance.

The study conducted by Rosli (2012) and Azeman (2012) was used as a basis by Liaw (2013) whereby the sinusoidal arrangement was modified. Moreover, both of the previous studies were closer to the range of nanoscale instead microscale. The horizontal length of the channel is fixed constant at 10 cm with an addition of sum of 1.0 cm for inlet and outlet channel. The microchannel studied by Rosli (2012) was modified such that the diameter was increased to 100 μm from 10 μm . Liaw (2013) main parameter of interest was the number of cyclic turns. This project shall continue the work of Rosli (2012), Azeman (2012) and Liaw (2013) whereby the overall geometric design will be modified.

CHAPTER 3

METHODOLOGY

3. METHODOLOGY

3.1 Research Methodology

The objective of this study is to investigate the hydrodynamics of the mixing of nitrogen and hydrogen gases in various geometry configuration of a microchannel to embed catalyst for ammonia synthesis by using CFD simulation and modeling. This project involves familiarization with microfluidic technology and usage of Computational Fluid Dynamics to simulate the mixing effect in the microchannel. The study utilizes ANSYS CFX 14.5 to run the CFD simulation.

The three major phase of this study includes the development of geometry, mesh generation and computational processing. The geometry of the microchannel is produced by using ANSYS Design Modeler. The general design based on studies conducted by Rosli (2012), Azeman (2012) and Liaw (2013) is modified in terms of geometry configuration as a continuation of their work. Periodic changes in geometry can induce spatially periodic flow which is necessary to create chaotic advection in passive micromixer (Nguyen, 2008). In this project, at least two different geometry configurations will be tested. Both geometries differ in terms of the geometry of their mixing unit.

The general properties of each microchannel to be applied in this study are outlined as in the following:

Total Length of Geometry	= 11cm
Total Width of Geometry	= 5 cm
Diameter of Channel	= 100 μ m
Number of Cycle(s)	= 10 cycles

Figure 12 and Figure 13 shows both proposed geometry configurations that is studied in this project.

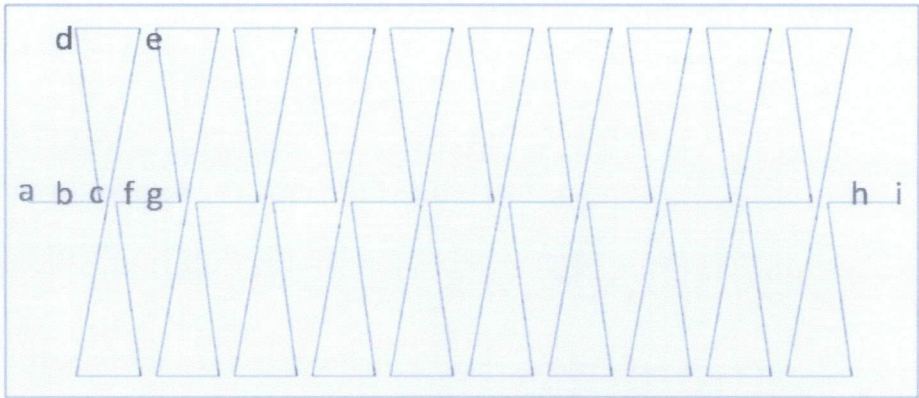


Figure 12 Geometry Configuration A

Total Length of geometry (a – i)	= 11.0 cm
Inlet/ Outlet Length (a – b/ h – i)	= 0.5 cm
Length of 1 Cycle (b – g)	= 1.0 cm
b – c/ f – g	= 0.4 cm
c – f	= 0.2cm
d – e	= 0.8 cm

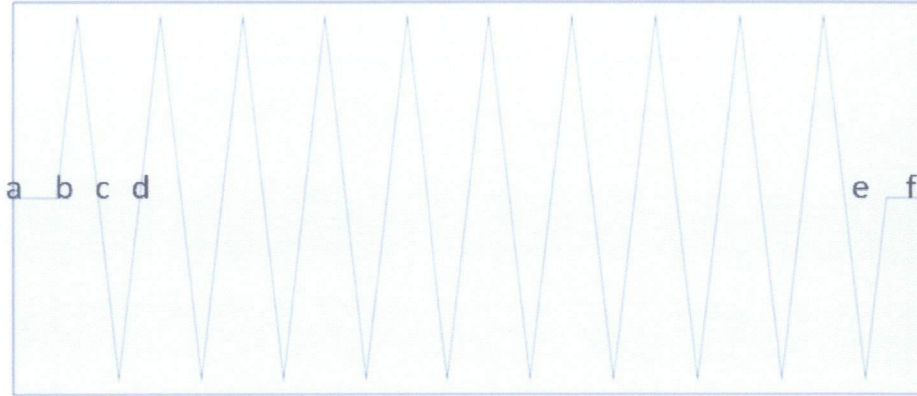


Figure 13 Geometry Configuration B

Total Length of Geometry (a – f)	= 11.0 cm
Inlet/ Outlet Length (a – b/ e – f)	= 0.5 cm
Length of 1 Cycle (b – d)	= 1.0 cm
b – c	= 0.5 cm

After geometry creation, mesh will be generated by using ANSYS Meshing. Mesh generation is one of the many critical aspects of CFD simulation. Meshing properties are specified to obtain the most appropriate mesh quality capable to produce results with high accuracy. In this study, the number of nodes, elements and orthogonal quality will be taken into consideration to evaluate the quality of the meshing. The orthogonal quality is one of the mesh metrics available in ANSYS Meshing. It is considered as to see the grid quality in terms of the angle at the point of intersection between cells. The angle nearing to 90° between the cells give a better distribution among the cells in the grid. Generally, the orthogonal quality is kept to a minimum of 0.05. The best cells will have an orthogonal quality converging to 1. In this project, two sets of meshes were generated based on both geometry designs. Through analysis, the selected meshing property is then used to analyze the flow behavior of both gas components.

In the next step, the computational processing will be conducted on the flow of N₂ and H₂ inside the microchannel. The simulation is run based on the boundary condition and

the fluid parameters set up in the Pre – CFX section. The following summarizes the pre – processing details.

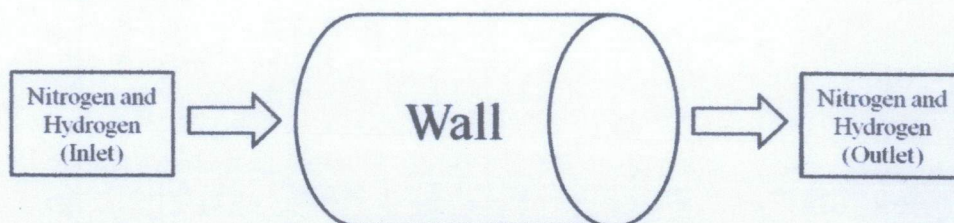


Figure 14 Boundary Conditions

Table 3 Domain Physics

Domain Physics for CFX		
Domain - Default Domain		
Type	Fluid	
Location	B77	
Materials	H ₂ at STP	N ₂ at STP
Fluid Definition	Material Library	Material Library
Morphology	Continuous Fluid	Continuous Fluid
Minimum Volume Fraction	0.75	0.25
Settings		
Buoyancy Model	Non Buoyant	
Domain Motion	Stationary	
Reference Pressure	1 atm	
Heat Transfer Model	Isothermal	
Fluid Temperature	25°C	
Homogeneous Model	On	
Turbulence Model	k-ε model	
Turbulent Wall Functions	Scalable	

Table 4 Boundary Physics

Boundary Physics for CFX			
Domain	Boundaries		
Default Domain	Boundary - Inlet		
	Type	INLET	
	Location	INLET	
	Settings		
	Flow Regime	Subsonic	
	Mass And Momentum	Normal Speed	3.33 m/s
	Turbulence	Medium Intensity and Eddy Viscosity Ratio	
	Fluid	Hydrogen	Nitrogen
	Volume Fraction	0.75	0.25
	Boundary – Outlet		
	Type	OUTLET	
	Location	OUTLET	
	Settings		
	Flow Regime	Subsonic	
	Mass And Momentum	Average Static Pressure	
	Pressure Profile Blend	0.05	
	Relative Pressure	0 Pa	
	Pressure Averaging	Average Over Whole Outlet	
	Boundary – Wall		
	Type	WALL	
	Location	WALL	
	Settings		
	Mass And Momentum	No Slip Wall	
	Wall Roughness	Smooth Wall	

Table 5 Solver Control

Solver Control	
Advection Setting	High Resolution
Turbulence Numeric	First Order
Convergence Control	
Min. Iterations	1
Max. Iterations	100
Fluid Timescale Control	
Timescale Control	Auto Timescale
Length Scale Option	Conservative
Timescale Factor	0.0001
Convergence Criteria	
Residual Type	RMS
Residual Target	0.000001

Next, the simulation will be run at the Solver Manager Section. The governing equation for CFD simulation is the Navier - Stokes equation which is described as following:

$$\rho \left(\frac{\partial \mathbf{v}}{\partial t} + \mathbf{v} \cdot \nabla \mathbf{v} \right) = -\nabla p + \nabla \cdot \mathbf{T} + \mathbf{f} \quad (3)$$

Where

\mathbf{v} = flow velocity;

ρ = fluid density;

p = pressure;

\mathbf{T} = deviatoric component of the stress tensor;

\mathbf{f} = body forces (per unit volume) acting on the fluid.

In this project, the flow regime is assumed as subsonic. Azeman (2012) reported the Mach number at the inlet and throughout the microchannel at 0.01 and 0.02 respectively. Since the value is less than 0.03, the gas flow in this system is considered incompressible. The constant flow of an incompressible Newtonian fluid in microchannel can be described by the following Navier-Stokes and Continuity Equation:

For incompressible fluid, the continuity equation is

$$\frac{\partial v_k}{\partial x_k} = 0 \quad (4)$$

The momentum equation is

$$\frac{\partial(\rho v_j v_k)}{\partial x_j} = \frac{\partial}{\partial x_j} \left(-p \delta_{ij} + \mu \left(\frac{\partial v_i}{\partial x_j} + \frac{\partial v_j}{\partial x_i} \right) \right) = \rho g_i \quad (5)$$

Where

X = Cartesian coordinate direction;

i, j, k = Cartesian axis;

$\delta_{ij} = 1$ if $i = j$ and 0 if otherwise;

μ = dynamic viscosity.

In addition, the species distribution follows the diffusion convective equation with assumption of non-slip boundaries as follows:

$$\frac{\partial c}{\partial t} + \frac{\partial v_k(c)}{\partial x_k} = D \frac{\partial^2 c}{\partial x^2} \quad (6)$$

Where

c = concentration;

t = time; D = diffusivity.

The software will solve the discretized conservation equation in an iterative manner until it converges to one value. The accuracy of a converged solution depends on the accuracy of the developed geometry, the meshing quality, the assumptions made and additional numerical errors.

Finally, in post-processing, ANSYS provides a set of post – processing tools to display the results of the simulation. Users can obtain detailed results over selected parts of the geometry. The results can be exported as text data or spreadsheet for further calculations. Based on analysis of these data, the parameters can be manipulated in order to perform design optimization. In this study, parameters such as velocity and pressure drop will be taken into consideration.

3.2 Tools

The tool applied in this CFD simulation study is ANSYS CFX 14.5.

3.3 Key Milestones

Project timeline for both FYP 1 and FYP 2 are attached in Appendix 1 and 2 respectively.

CHAPTER 4

RESULTS AND DISCUSSION

4. RESULTS AND DISCUSSION

4.1 Mesh Sensitivity Study

After successfully developing both geometry configuration A and B through ANSYS Design Modeler, the project proceeds with mesh generation. By using ANSYS Meshing to generate the mesh, several mesh properties were manipulated to obtain satisfactory number of nodes, elements and orthogonal quality. The following summarized the mesh that was successfully created for both geometry configurations.

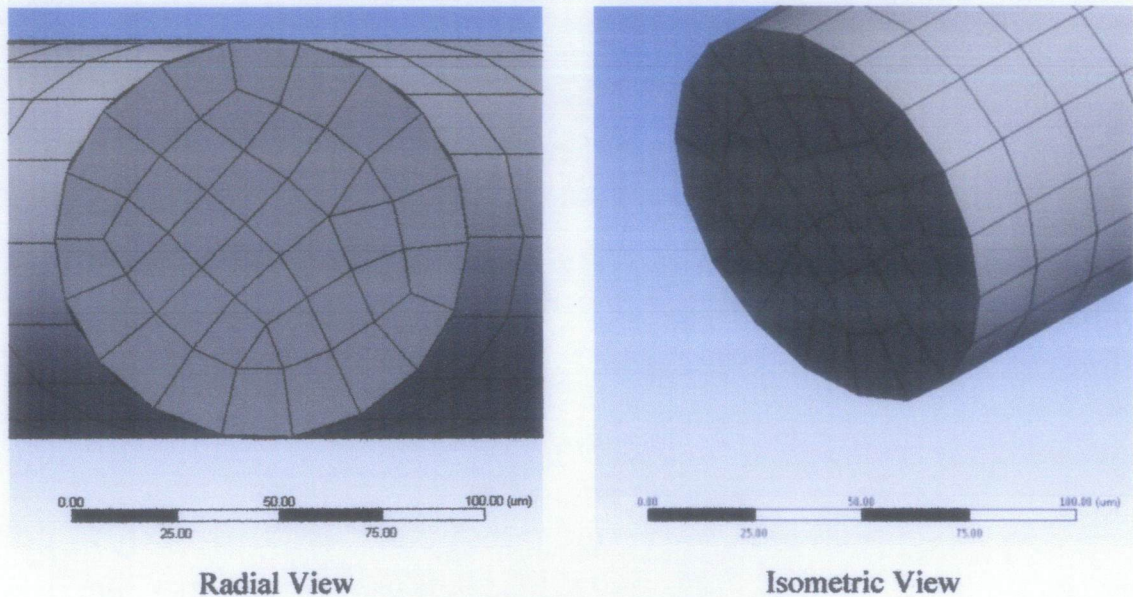
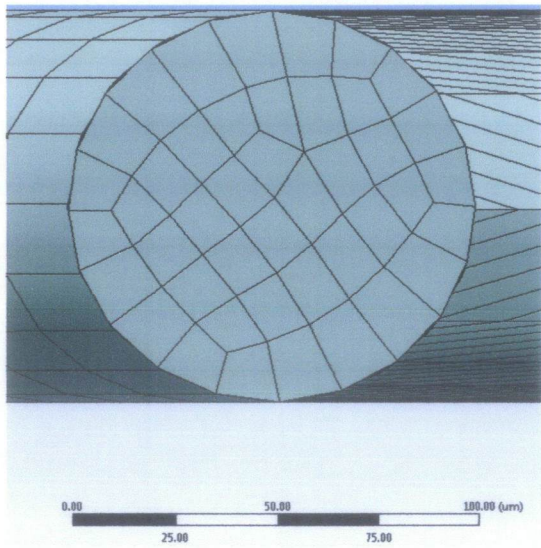
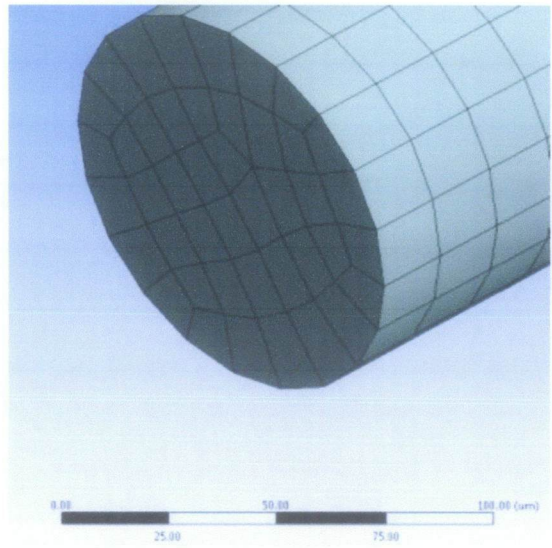


Figure 15 Mesh 1 Design A

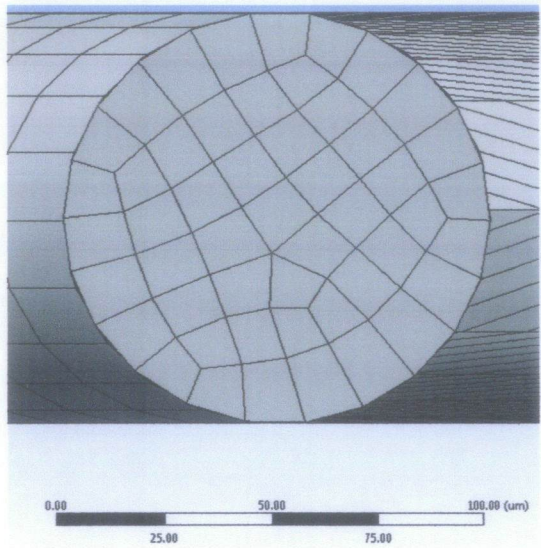


Radial View

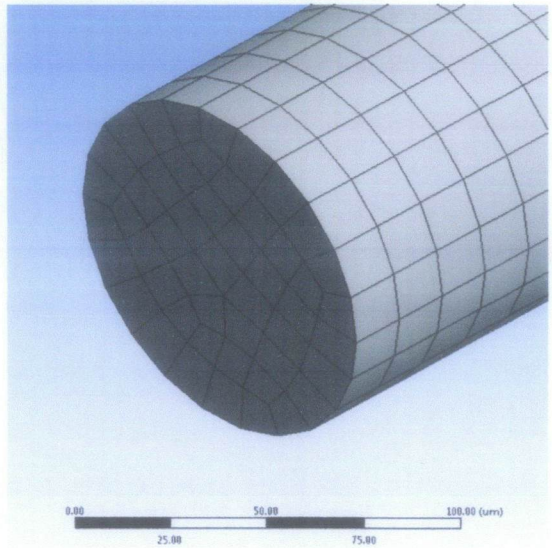


Isometric View

Figure 16 Mesh 1 Design B



Radial View



Isometric View

Figure 17 Mesh 2 Design B

Table 6 Completed Meshing Properties

Mesh	Geometry	Number of Nodes	Number of Elements	Simulation Duration
1	A	3091728	2511990	9 hours 18 minutes
	B	2990736	2381469	11 hours 22 minutes
2	B	4038370	3256700	16 hours 26 minutes

Based on Table 6, it is observed by comparing mesh 1 and mesh 2 of design B that the better mesh quality would produce higher number of nodes. However, finer mesh would take longer simulation time. A decent quality of mesh 2 for design A was not successfully generated and hence will not be compared in this report. However, it is expected that similar outcomes would be observed.

A comparison of contour plot for design B is summarized as following.

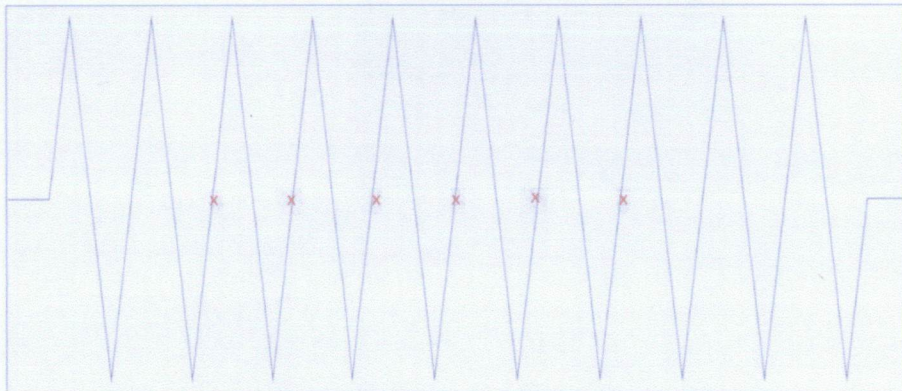
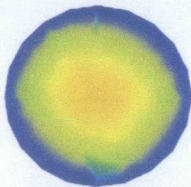
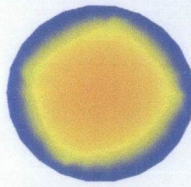
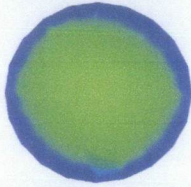
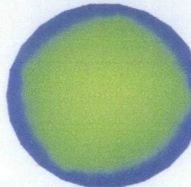
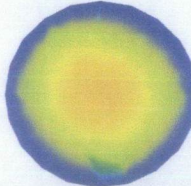
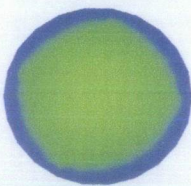
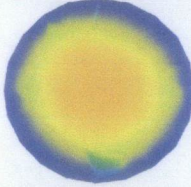
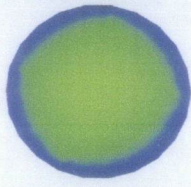
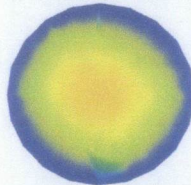
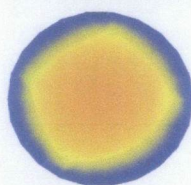
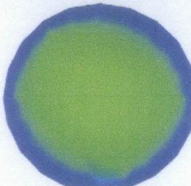
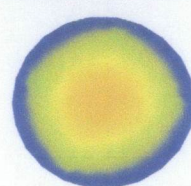


Figure 18 Location of Comparison

The table show the comparison of the velocity contour with their respective location coordinates.

Table 7 Comparison of velocity contour plot

Coordinates (x,y,z)	Mesh 1	Mesh 2
(0, 0, 0.02)		
(0, 0, 0.03)		
(0, 0, 0.04)		
(0, 0, 0.05)		
(0, 0, 0.06)		
(0, 0, 0.07)		

It is observed that the fluid flow in mesh 1 and mesh 2 is not uniform radially throughout the circular tube as there are several visible uneven contours near the edge. However, mesh 2 is more refined showing less jagged contours compared to mesh 1 at the same location. The lack of uniformity is due to insufficiently refined mesh, thereby limiting its accuracy. Therefore, mesh should be further refined to produce a smoother contour plot and increases reliability of the result. The mesh with higher refinement quality was unable to be generated and tested due to unsuccessful manipulation of mesh properties. Hence, results of this project will only be discussed based on the most refined mesh available which is mesh 2.

The following figure shows the comparison of nitrogen outlet velocity along y – axis for both mesh quality of design B. In this nitrogen enter the microchannel at a speed of 3.33 m/s, and is expected to exit the channel at similar speed. From the figure, it is observed that for both mesh quality, nitrogen exits at a speed at the range of 3.33 m/s. However it is noted that the speed is lower as it approaches the side wall. This is resulted by the no – slip boundary condition that was assumed in the earlier section.

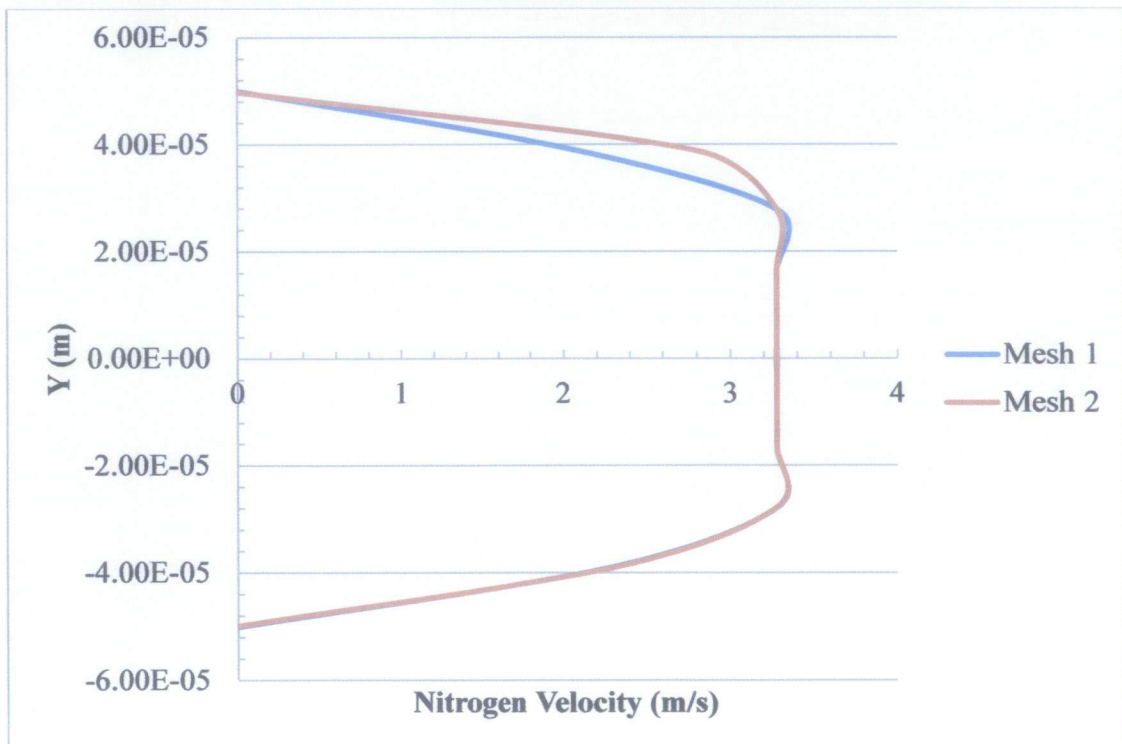


Figure 19 Nitrogen Velocity Profile

The current sensitivity study showed that quality of meshes is indeed crucial in producing reliable and accurate results. A refined mesh is absolutely necessary so that the solver is able to compute the solution to higher accuracy. Moreover, accuracy of computed solution also depends on assumptions made.

4.2 Analysis of Velocity of Gas Components

After completed meshing, the flow simulation was conducted through ANSYS CFX 14.5. The following discussed the results of gas flow behaviour for both geometry design A and B.

4.2.1 Geometry Design A

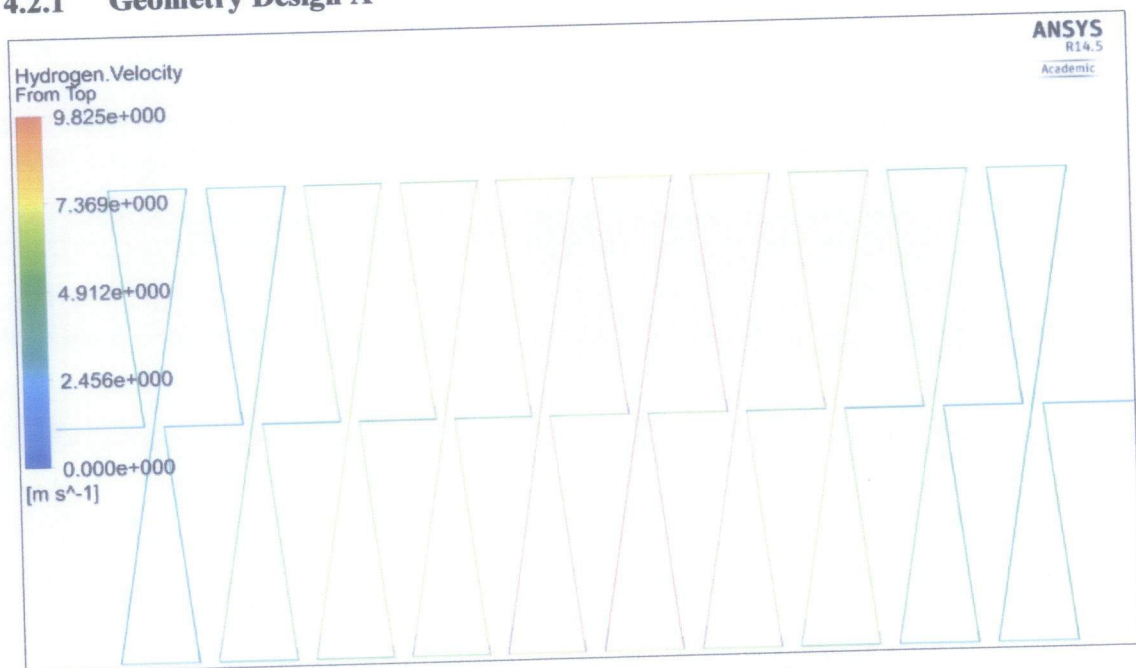


Figure 20 Axial Hydrogen Velocity for Design A

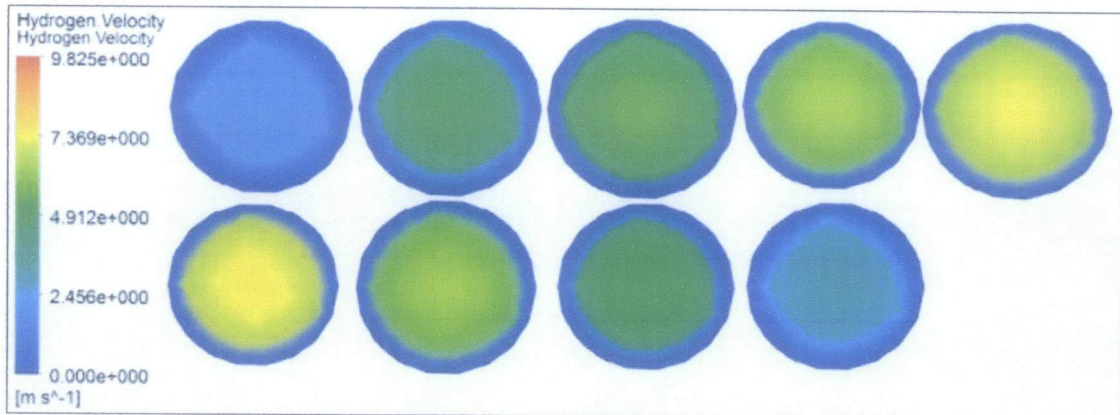


Figure 21 Radial Hydrogen Velocity for Design A after End of Each Consecutive Period of Mixing Unit



Figure 22 Axial Nitrogen Velocity for Design A

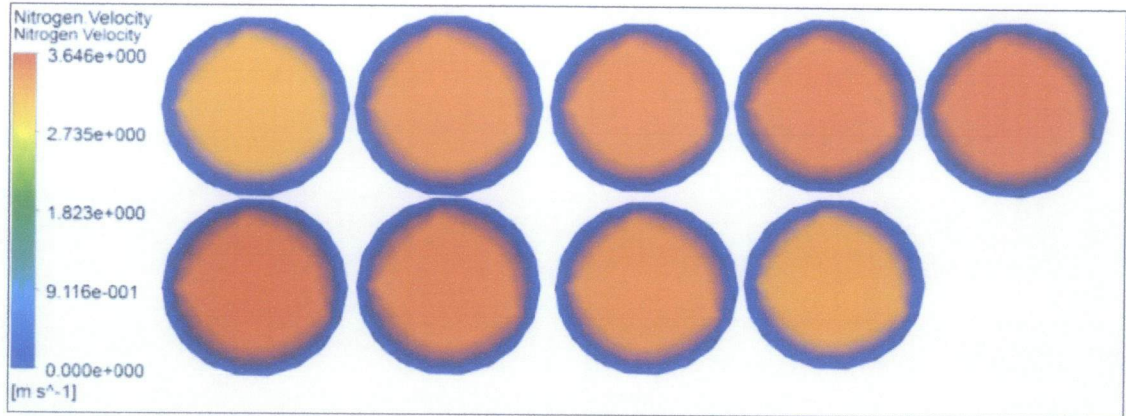


Figure 23 Radial Nitrogen Velocity for Design A after End of Each Consecutive Period of Mixing Unit

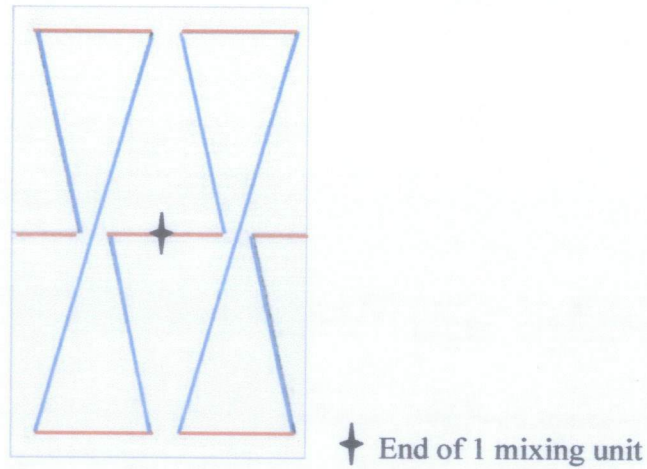


Figure 24 Segment of Microchannel Design A

Figure 20 and Figure 22 shows the axial velocity of hydrogen and nitrogen gas component respectively. Figure 24 shows a segment of the microchannel consisting of two mixing units. The lines highlighted red in Figure 24 shows the short sections of the mixing unit whereas the lines highlighted blue shows the long sections of the mixing units respectively.

It can be seen that the flow of nitrogen is faster at the short sections of the mixing unit but slows down as it flows through the long section of the mixing unit. It is also observed that hydrogen velocity flows faster in the midsection of the microchannel compared to the more stable flow of the nitrogen component. Due to larger molecular weight, nitrogen flow is more stable compared to hydrogen. In addition, it is found that

the flows of both gas components are approximately equal at the short sections of every mixing unit.

Figure 21 and Figure 23 shows the radial velocity of both gas components respectively as it exits each mixing unit. It is seen that generally both gases have higher velocity in the middle of the circular channel. This is due to the no slip boundary condition set on the walls of the channel in the CFX Pre section. For both gases, the flow is almost uniform throughout the microchannel.

4.2.2 Geometry Configuration B

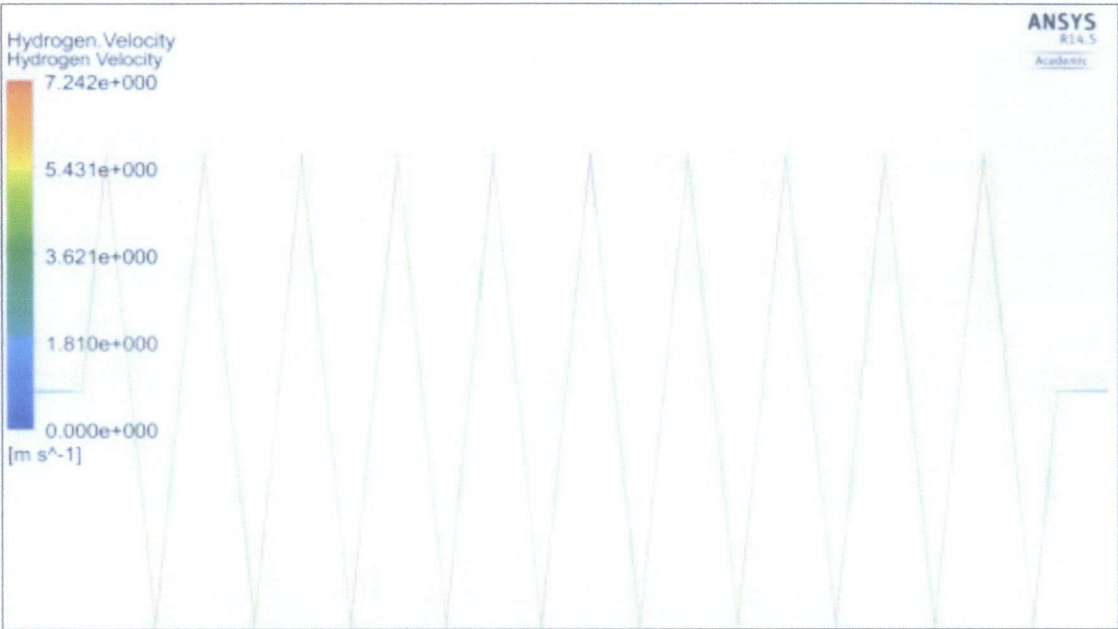


Figure 25 Axial Hydrogen Velocity for Design B

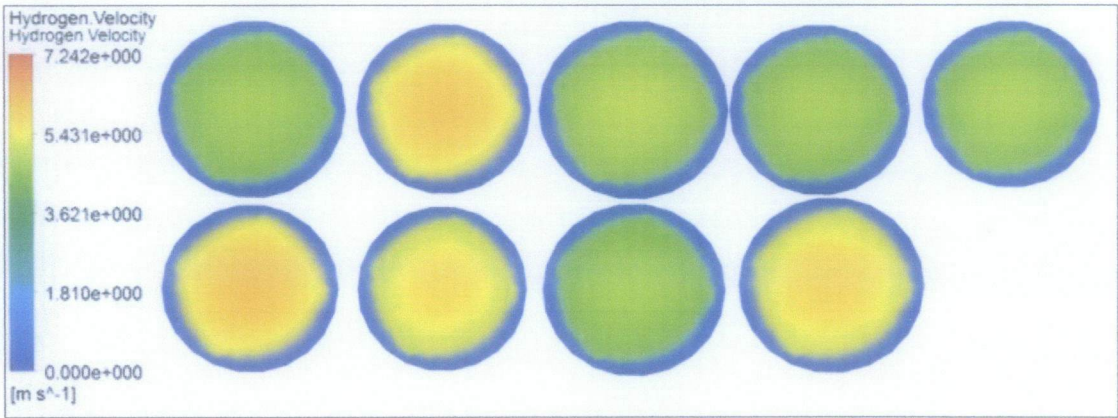


Figure 26 Radial Hydrogen Velocity for Design B after End of Each Consecutive Period of Mixing Unit



Figure 27 Axial Nitrogen Velocity for Design B

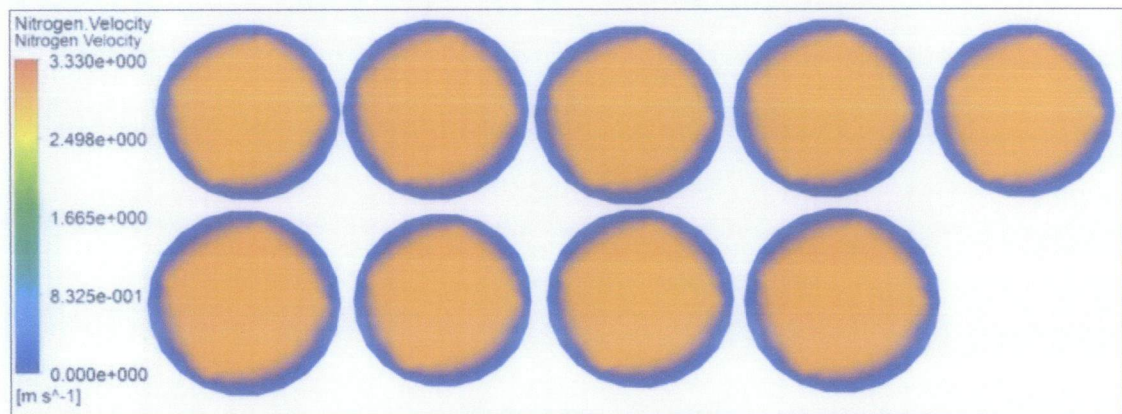


Figure 28 Radial Nitrogen Velocity for Design B after End of Each Consecutive Period of Mixing Unit

Figure 25 and Figure 27 shows the axial velocity of hydrogen and nitrogen gas components respectively. The flow of hydrogen gas component is non – uniform axially across the microchannel. Significant velocity change is observed before and after successive bends at every section of the microchannel. Nitrogen gas component on the other hand is observed to flow in a more uniform manner across the microchannel. Very little change in velocity is observed after every bends. Similarly, as nitrogen has larger

molecular weight, it is expected that the flow would be more stable compared to hydrogen.

Figure 26 and Figure 28 shows the radial velocity of hydrogen and nitrogen gas components respectively. Similar to observation in geometry A, both gas components flow faster in the middle section of the circular channel and the flow is uniform throughout the microchannel.

The flow of both gas components were probably affected by laminar recirculation induced by the zigzag angles as described by Mengeaud et al (2002) in his paper. The channel wall after each angle acts as an obstacle thereby reducing the flow lines along the walls and an increase in local velocity. Hence, the velocity tends to increase after each angle.

4.3 Pressure Differences in Microchannel

As microchannel is also a very long tube, it has high probability to experience pressure drop. This pressure drop occurs with frictional forces, caused by the resistance of the fluid to flow. Moreover, the existence of many turns and bends also contributes to the pressure drop.

Pressure drop across a microchannel can be evaluated from the following equation (Schlichting, 1979):

$$\Delta P = \frac{V^2 \times f \times L \times \rho}{2D} \quad (7)$$

Where

V = Velocity of fluid

f = Friction factor = $\frac{64}{Re}$ (For laminar flow)

L = Length of microchannel

ρ = Density of fluid

D = Diameter of microchannel

Figure 31 illustrates the linearized pressure profile of both geometry design A and B.

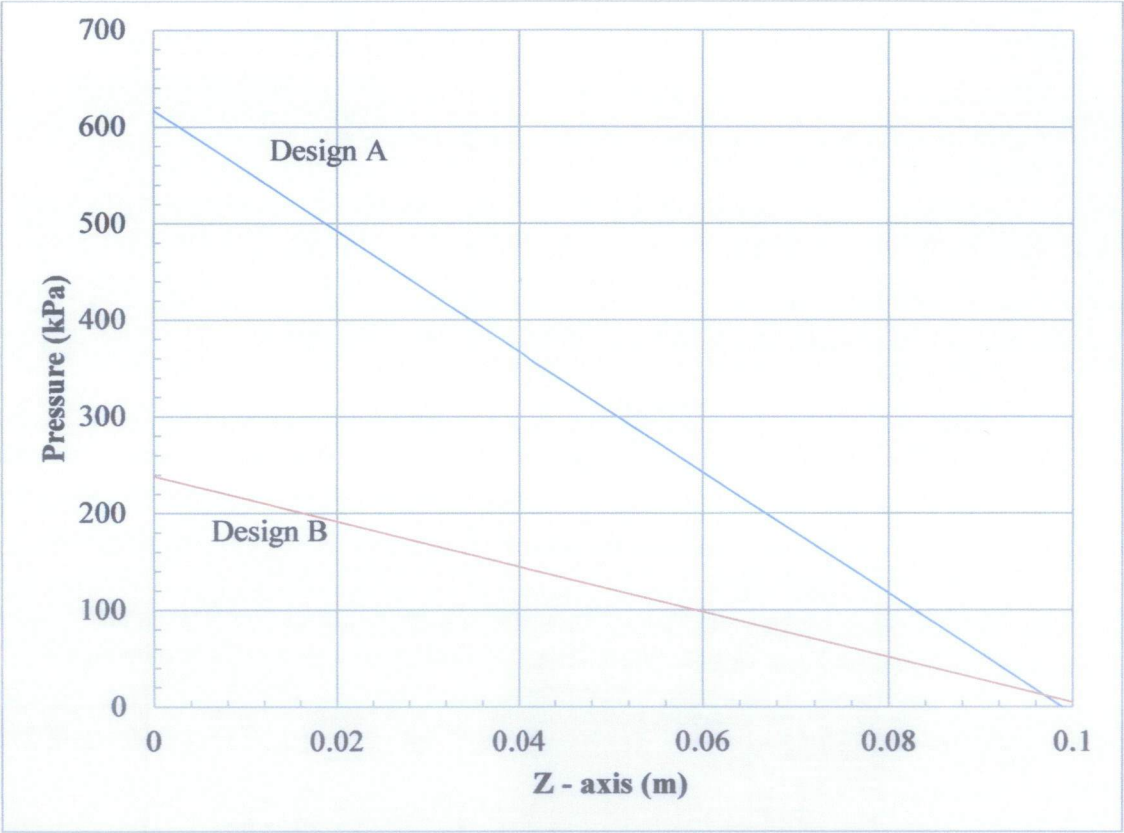


Figure 29 Pressure Profile along the Microchannel

It is found that geometry design A experiences a much higher pressure difference compared to geometry design B. A contributing factor may due to the effective length of microchannel design A is longer than design B. Moreover the different geometry of the mixing unit in both designs may also contribute to the magnitude of pressure difference. Geometry design A has doubled the number of bends compared to design B.

CHAPTER 5

CONCLUSION AND RECOMMENDATION

5. CONCLUSION

In this project, computational fluid dynamics was applied to study the hydrodynamics of mixing between Ammonia reactant gases in various geometry configurations of a microchannel. By studying the hydrodynamics of mixing, it will assist to determine the optimum localization of catalyst for ammonia synthesis in the next stage of the project.

However, in this stage of the study, the reaction between nitrogen and hydrogen gas components are not being included. Two geometry configurations were developed and tested. Current observation of this project utilizes results from one meshing quality for both designs. However, continuation would involve usage of meshes of higher quality to ensure reliability and accuracy of results.

Further analysis on current mesh quality indicates that both geometry configurations illustrate a very different flow pattern for both gas components. Flow of hydrogen components is at higher velocity in the midsection of geometry A whereas the velocity changes are observed at every bend of geometry B. As for nitrogen component, geometry A exhibits a pattern of high velocity at short paths, and lower velocity at longer paths. Geometry B on the other hand, exhibits a more uniform flow with less significant velocity change after every zigzag bends.

Based on this study, it is proposed for geometry A, the catalyst should be localized throughout the microchannel but concentrated more on the short sections of the mixing unit in the microchannel where both components are observed to be flowing at an almost equal velocity. It is expected that reaction with nitrogen will occur more rapidly. As for

radial view, current observation indicates both gas components flow uniformly across the diameter of the microchannel. Hence, catalyst thickness should be localized evenly throughout the reactor. Catalyst thickness should be sufficient to be in contact with mixing gases. As for geometry B, catalyst may be localized throughout the microchannel concentrating on the location with more stable flow of fluids which is between two successive bends. Both geometry configurations have potential and limitations. Yet, in terms of pressure drop, it is found that geometry design B is more preferable due to much lower pressure drop.

The prospect of this project is very useful for future developments. As there are no really rules of thumb in designing microreactor, more parameters should be studied in order to be able to come up with an optimum design. With an optimum design, the project may proceed with the next stage of including chemical reaction to synthesize ammonia.

Due to unsuccessful manipulation of mesh properties, the more refined mesh was unable to be generated and tested. Hence, further study should include simulation conducted with more refined mesh. Besides that, study could be continued with modification on the suggested designs to a more curved arc bends rather than sharp bends, different angle of bends, study on number of periods of mixing unit, inflow configurations, and other possible geometry configuration.

REFERENCES

- Aubin, J., Fletcher, D. & Xuereb, C. (2005). Design of micromixers using CFD modelling. *Chemical Engineering Science*, 60(8), 2503--2516.
- Azeman, M.K. (2012). *CFD Modelling of the Microreactor for the Ammonia Synthesis*. Undergraduate. Universiti Teknologi PETRONAS.
- BASF SE (2013). Fertilizer out of thin air. [press release] 21 March 2013.
- Capretto, L., Cheng, W., Hill, M. and Zhang, X. (2011). Micromixing Within Microfluidic Devices. *Topics in Current Chemistry*, 304 pp. 27-68.
- E-education.psu.edu (2011). *Industrial Agriculture | GEOG 030: Geographic Perspectives on Sustainability and Human-Environment Systems, 2011*. [online] Retrieved from: <https://www.e-education.psu.edu/geog030/node/358> [Accessed: 21 June 2013].
- Fang, Y., Ye, Y., Shen, R., Zhu, P., Guo, R., Hu, Y. and Wu, L. (2012). Mixing enhancement by simple periodic geometric features in microchannels. *Chemical Engineering Journal*, 187 p. 306– 310.
- Harrison, J.A. (2003). "The Nitrogen Cycle: Of Microbes and Men," *Visionlearning* Vol. EAS-2 (4). [online] Retrieved from http://www.visionlearning.com/library/module_viewer.php?mid=98 [Accessed: 21 June 2013]
- Hsieh, S., & Huang, Y. (2008). Passive mixing in micro-channels with geometric variations through μ PIV and μ LIF measurements. *J.Micromech.Microeng.* 18, 1-11.
- Lee, C., Chang, C., Wang, Y. & Fu, L. (2011). Microfluidic mixing: a review. *International journal of molecular sciences*, 12 (5), 3263--3287.

- Liaw, I. (2013). *Investigation of the Flow Behavioral dynamics of Ammonia Component Gases in a Microreactor via CFD Approach*. Undergraduate. Universiti Teknologi PETRONAS.
- Jensen, K. (2001). Microreaction Engineering - Is smaller better?. *Chemical Engineering Science*, 56 (2), pp. 293 - 303.
- Koch, M., Evans, A. and Brunnschweiler, A. (2000). *Microfluidic technology and applications*. Philadelphia, PA: Research Studies Press.
- Mengeaud, V., Josser & Girault, H. (2002). Mixing processes in a zigzag microchannel: finite element simulations and optical study. *Analytical Chemistry*, 74 (16), 4279–4286.
- Mills, P., Quiram, D. and Ryley, J. (2007). Microreactor technology and process miniaturization for catalytic reactions—A perspective on recent developments and emerging technologies. *Chemical Engineering Science*, 62 (24), pp. 6992 - 7010.
- Nguyen, N. (2008). *Micromixers*. Norwich, NY: William Andrew.
- Nguyen, N. and Wereley, S. (2006). *Fundamentals and applications of microfluidics*. Boston: Artech House.
- Nguyen, N. and Wu, Z. 2005. Micromixers—a review. *Journal of Micromechanics and Microengineering*, 15 (2), p. 1.
- Park, H. (n.d.). *CFD Advantages and Practical Applications*. [online] Retrieved from: http://glumac01.nimbol.com/greenResources/GR_CFD_Advantages.html [Accessed: 21 June 2013].
- Patsis, G., Ninos, K., Mathioulakis, D. and Kaltsas, G. 2011. Simulation and Experimental Evaluation of Gas Mass Flow Transfer Rate in Microchannels. *Procedia Engineering*, 25 pp. 447–450.

- Potashcorp.com (2013). *Home - Industry Overview - PotashCorp.* [online] Retrieved from: <http://www.potashcorp.com/overview/nutrients/nitrogen/overview/world-uses-and-top-producers> [Accessed: 17 June 2013].
- Quiram, D., Hsing, I., Franza, A., Jensen, K. and Schmidt, M. (2013). Design issues for membrane-based, gas phase microchemical systems. *Chemical Engineering Science*, 55 (16), pp. 3065 - 3075.
- Reyhanian, M., Croizet, C. & Gatignol, R. (2011). Mixing Length in a Micro Channel. 1333 766.
- Rosli, M. (2012). *CFD Modelling of the Micromixing Process for the One-Step Magnetically Induced Urea Synthesis 1*. Undergraduate. Universiti Teknologi PETRONAS.
- Schlichting, H. (1979). *Boundary-layer theory*. New York: McGraw-Hill.
- Schrock, R. (2006). Nitrogen Fix. *MIT Technology Review*, Iss. v1.13.05.10.
- Sharipov, F. & Graur, I. (2012). Rarefied gas flow through a zigzag channel. *Vacuum*, 86 (11), 1778--1782.
- Tang, G., Li, Z., He, Y. and Tao, W. (2007). Experimental study of compressibility, roughness and rarefaction influences on microchannel flow. *International Journal of Heat and Mass Transfer*, 50 (11-12), pp. 2282-2295.
- Tsai, R. and Wu, C. (2011). An efficient micromixer based on multidirectional vortices due to baffles and channel curvature. *Biomicrofluidics*, 5 (014103).
- Wang, H., Iovenitti, P., Harvey, E. and Masood, S. (2003). Passive Mixing in Microchannels by Applying Geometric Variations. *Proceedings of SPIE*, 4982 pp. 282 - 289.
- Wang, H., Iovenitti, P., Harvey, E. and Masood, S. (2003). Passive Mixing in Microchannels by Applying Geometric Variations. *Proceedings of SPIE*, 4982 pp. 282 - 289.

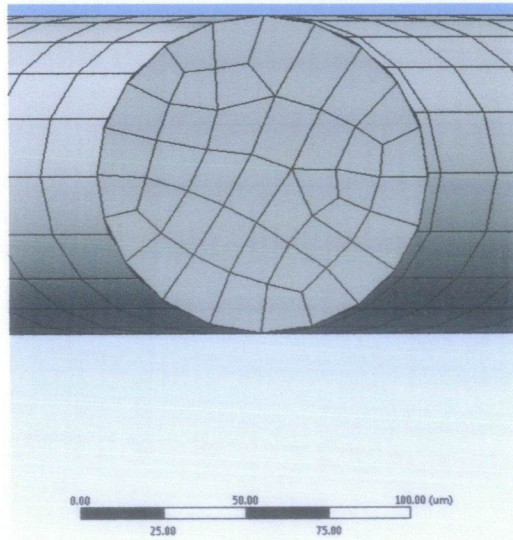
- Wang, M. and Li, Z. (2006). Gas mixing in microchannels using the direct simulation Monte Carlo method. *International Journal of Heat and Mass Transfer*, 49 (9 - 10), pp. 1696-1702.
- Yan, F. & Farouk, B. (2001). Prediction of mixing of two parallel gas streams in a microchannel using the direct simulation Monte Carlo method. 585 510.
- Zhang, Z., Yim, C. and Cao, X. (2008). Quantitative characterization of mixing simulation. *Biomicrofluidics*, 2 (034104).

APPENDIX 1: PROJECT TIMELINE FOR FYP 1

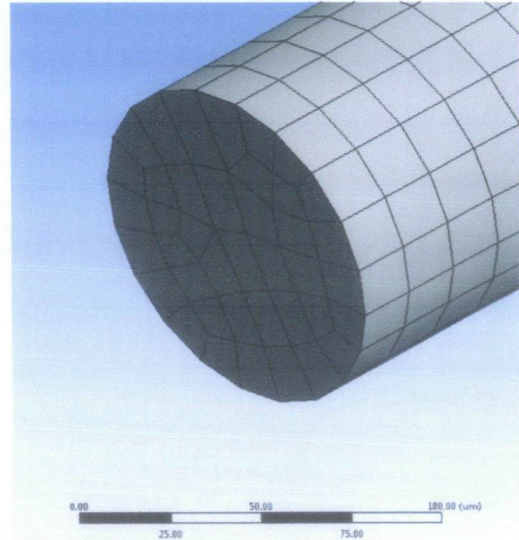
[illegible]

APPENDIX 3: GENERATED MESH

The following figures are some of the inferior quality meshes generated for design geometry A.

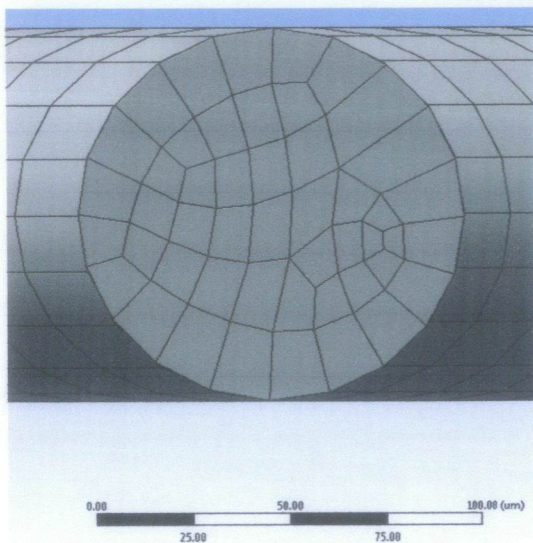


Radial View

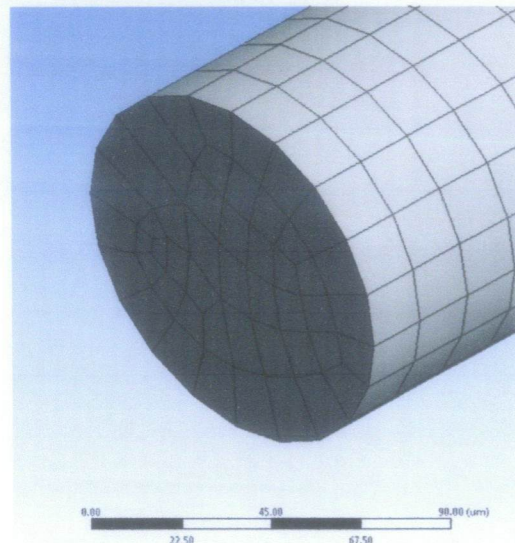


Isometric View

Figure 30 Mesh with 3694695 nodes



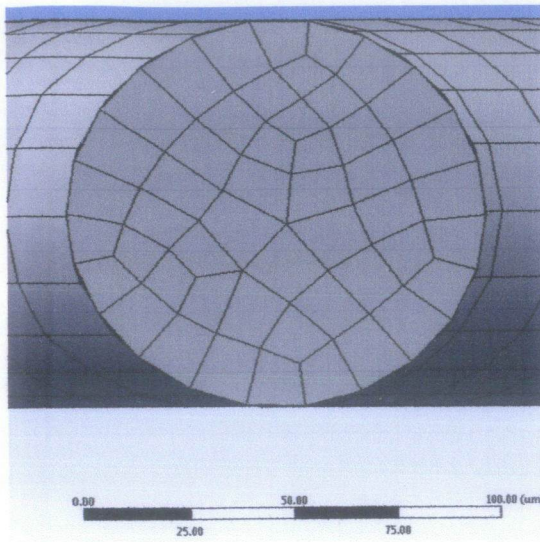
Radial View



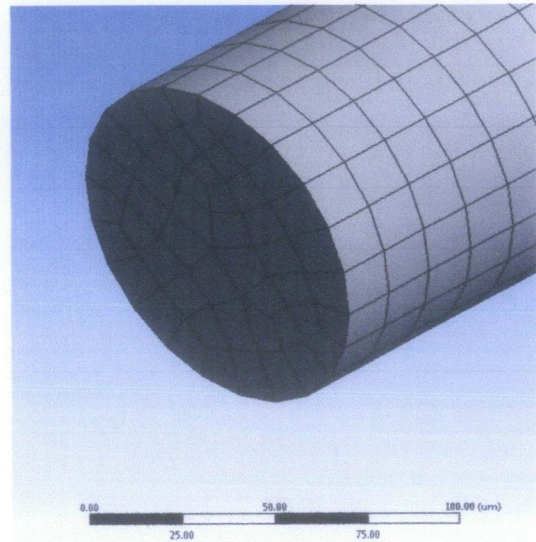
Isometric View

Figure 31 Mesh with 4512733 nodes

APPENDIX 3: GENERATED MESH (Continued)



Radial View



Isometric View

Figure 32 Mesh with 4911049 nodes